Heterogeneous viscoelasticity: a combined theory of dynamic and elastic heterogeneity

Walter Schirmacher[1,2,3], Giancarlo Ruocco[1], and Valerio Mazzone[1],
[1] *Dipartimento di Fisica, Universitá di Roma "La Sapienza", P'le Aldo Moro 2, I-00185, Roma, Italy,*
[2] *Institut für Physik, Universität Mainz, Staudinger Weg 7, D-55099 Mainz, Germany,*
[3] *Institut für Theoretische Physik, Leopold-Franzens-Universität Innsbruck, Technikerstraße 25/2, A-6020 Innsbruck, Austria*

We present a heterogeneous version of Maxwell's theory of viscoelasticity based on the assumption of spatially fluctuating local viscoelastic coefficients. The model is solved in coherent-potential approximation (CPA). The theory predicts an Arrhenius-type temperature dependence of the viscosity in the vanishing-frequency limit, independent of the distribution of the activation energies. It is shown that this activation energy is generally different from that of a diffusing particle with the same barrier-height distribution, which explains the violation of the Stokes-Einstein relation observed frequently in glasses. At finite, but low frequencies the theory describes low-temperature asymmetric alpha relaxation. As examples we report the good agreement obtained for selected inorganic, metallic and organic glasses. At high frequencies the theory reduces to heterogeneous elasticity theory, which explains the occurrance of the boson peak and related vibrational anomalies.

PACS numbers: 65.60.+a

The interplay between relaxation and elasticity in very viscous glass-forming supercooled liquids has been in the focus of glass scientists since the pioneering work of Maxwell on visco-elasticity [1]. Within Maxwell's theory the glass transition is a very simple matter. The relaxation time is given by $\tau = \eta/G_\infty$, where $\eta = \eta(T)$ is the shear viscosity and G_∞ is the high-frequency shear modulus. If this quantity is (much) larger than the observation time or the typical time for glassblower's manipulations the material has transformed effectively to a solid. Within Maxwell's theory the loss part of the frequency-dependent shear modulus exhibits a Debye peak of the form $G''(\omega) = \eta\omega/(1+\omega^2\tau^2)$, which gives a peak at the frequency τ^{-1}. The peak positions of mechanical and dielectrical response spectra exhibit the same temperature dependence as the inverse viscosity, which varies exponentially with the inverse temperature as $\eta(T) \propto E_{\rm A}(T)/k_BT$. Near and above the glass transition temperature T_g (defined in the above way) the differential activation energy $E_{\rm A}$ follows a Vogel-Fulcher-Tammann law $E_{\rm A} \propto T/(T-T_0)$. At lower temperatures it levels off towards a temperature-independent value. There is some evidence that this temperature dependence of $E_{\rm A}$ is very similar to that of the shear modulus [2–4]. The idea behind this finding is that activation barriers are related via the yield stress to the shear stiffness [5]. The ratio between the low- high-temperature activation energies may serve as a measure of Angell's fragility classification. It is 1 for "strong" materials and up to 4 for "fragile" materials [6, 7]. In fragile glasses the elastic and dielectric loss peaks (α peaks), however, do not have the above Debye form but are broadened on a logarithmic frequency scale, which is called "stretching" [13]. The alpha peak in the low-temperature regime below T_g becomes quite asymmetric [8–12]. In this temperature regime the stretched alpha peaks have been described with phenomenological formulas like the Cole-Davidson or Kohlrausch equations [13].

Above the glass transition the mode-coupling theory (MCT) [14–16] gives a convincing and detailed account of the stretching phenomenon plus an anomalous increase beyond the alpha peak (short-time β relaxation). The glass transition T_c predicted by MCT is located somewhat above T_g. This ideal glass transition is described as an ergodicity-breaking transition with a corresponding divergence of the viscosity according to $\eta \propto [T-T_c]^{-\gamma}$, which describes the temperature dependencd of fragile glasses above T_c as well as the VFT law. Below T_c real glasses do not show a divergence of the viscosity, but the crossover to the high-E_A activation law. The activation energy of the viscosity in this regime is not equal to that of the diffusivity, a phenomenon, which has been called *Stokes-Einstein violation* [17, 18] for which an explanation will be given in the present treatment. There is evidence that in this temperature regime relaxation processes are governed by a free-energy "landscape", implying a broad distribution of activation barriers, which have to be overcome for single relaxational steps [19–21]. This spatial heterogeneity of activation barriers implies a strong heterogeneity of the local relaxation processes (*dynamical or relaxational heterogeneity*). Dynamical heterogeneities are not only visible in the relaxation spectra but also in the vibrational spectra (*elastic heterogeneity*), leading to vibrational anomalies, which violate the prediction of Debyes predictions based on elasticity theory [22–26].

In the present treatment, which addresses the temperature regime near and below T_g, we assume that the dynamical heterogeneities are frozen in. Contrary to other treatments based on such an assumption [27–29], we do not assume that the relaxation processes occur in parallel. To achieve this goal we use the CPA [30–32], which is known to capture the percolation aspects, which are inherent in heterogeneous transport: The conductivity of a strongly heterogeneous system is neither obtained by averaging over the microscopic resistances (series equiva-

lent circuit), nor by averaging the conductances (parallel equivalent circuit), but the current follows the percolative path of least resistance.

Applying our theory to both the heterogeneous viscosity and diffusivity problem we are able to put our finger on the fact that these dynamical problems involve different percolative aspects, which then lead to the Stokes-Einstein violation. These aspects have been addressed indirectly recently by the hard-sphere glass-transition theory [33].

At finite frequencies our heterogeneous viscoelastic CPA theory develops its power in describing the strong asymmetry of the α relaxation peak in terms of the distribution of the free-energy barriers. The increase of the loss modulus on the low-frequency side of the α peak as $G''(\omega) \propto \eta(T)\omega$ and hence its time-temperature superposition behavior is included automatically. The high-frequency part of the alpha maximum is non-universal in accordance with experiment. It reflects the details of the barrier distribution of the material, as anticipated by the seminal ideas of Goldstein [19] and Johari [8].

At very high frequencies, i.e. below and near the Debye frequency, our theory reduces to the CPA version of heterogeneous elasticity theory, which accounts for the vibrational anomalies of glasses [32].

We now start the description of our model in detail. We consider a visco-elastic fluid in which both the viscosity $\eta(\mathbf{r})$ and the high-frequency shear modulus $G(\mathbf{r})$ are assumed to vary in space. The local viscosity is assumed to be governed by a local free energy $\ln[\eta(\mathbf{r})/\eta_0] = F(\mathbf{r})/k_BT$ with $F(\mathbf{r}) = E(\mathbf{r}) - TS(\mathbf{r})$. E is the local energy barrier and S is a multi-excitation entropy [34, 35], which is related to E by a compensation (Meyer-Neldel) rule [34–37] $S(\mathbf{r})/k_B = \alpha E(\mathbf{r})$, so that we have $\eta(\mathbf{r}) = \eta_0 e^{\beta_{\rm eff} E(\mathbf{r})}$ with $\beta_{\rm eff} = [k_BT]^{-1} - \alpha$. The activation barrier, in turn, is assumed [3, 4] to be related by $E(\mathbf{r}) = VG(\mathbf{r})$ to the local high-frequency shear modulus, where V is an activation volume. The spatial fluctuations of E are assumed to be statistically independent, i.e. we work in terms of a coarse-grained model over volumina of size ξ, which is the correlation length of the fluctuations [32]. The statistics is then given by a common density $P(E_i)$, where E_i is the average value of $E(\mathbf{r})$ inside a coarse-graining volume, centered at $\mathbf{r}_i$.

We start working out our theory by writing down the linear Navier-Stokes equations in frequency space ($\partial/\partial t \to s = -i\omega + \epsilon$) for this model:

$$s\rho_m v_\ell(\mathbf{r},s) = \frac{K}{s}\nabla_\ell \nabla\cdot\mathbf{v} + 2\sum_j \nabla_j \eta_{\rm eff}(\mathbf{r},s)\hat{\mathcal{V}}_{\ell j}(\mathbf{r},s) \quad (1)$$

$v_\ell(\mathbf{r},s)$ are the Cartesian coefficients of the Eulerian velocity field, K is the bulk modulus [38], and $\widehat{\mathcal{V}}$ is the traceless shear strain rate tensor $\widehat{\mathcal{V}}_{\ell j} = \mathcal{V}_{\ell j} - \frac{1}{3}{\rm Tr}\{\mathcal{V}\delta_{\ell j}\}$ with $\mathcal{V}_{\ell j} = \frac{1}{2}\big(\nabla_\ell v_j + \nabla_j v_\ell\big)$. The space-dependent Maxwellian visco-elastic term is given by

$$\frac{1}{\eta_{\rm eff}(\mathbf{r},s)} = \frac{s}{G_{\rm eff}(\mathbf{r},s)} = \frac{1}{\eta(\mathbf{r})} + \frac{s}{G(\mathbf{r})} \quad (2)$$

Replacing in Eq. (1) $\eta_{\rm eff}$ by $G_{\rm eff}/s$ and v_i by su_i, where u_i are the dynamic displacements, one obtains equations of motions of linear elasticity with a space and frequency dependent shear modulus. These equations can be solved approximately in coherent-potential approximation [32] (CPA), giving a macroscopic frequency-dependent shear modulus $G(\omega) = s\eta(\omega) = G'(\omega) - iG''(\omega)$, where $G'(\omega) = \omega\eta''(\omega)$ is the storage modulus and $G''(\omega) = \omega\eta'(\omega)$ is the loss modulus. $\eta(s) = \eta'(\omega) + i\eta''(\omega)$, is the frequency-dependent viscosity. The self-consistent CPA equations for $\eta(s)$ are [32]

$$\eta(s) = \left\langle \frac{\eta^{(i)}_{\rm eff}(s)}{1 + \frac{\widetilde{\nu}}{3}\big(\eta^{(i)}_{\rm eff}(s) - \eta(s)\big)\Lambda_\eta(s)} \right\rangle_i \quad (3a)$$

$$\Lambda_\eta(s) = \frac{3}{k_\xi^3}\int_0^{k_\xi} dk k^2 \bigg(\frac{\frac{4}{3}sk^2}{s^2 + \big[K + \frac{4}{3}s\eta(s)\big]k^2} + \frac{2k^2}{s + \eta(s)k^2}\bigg) \stackrel{s\to 0}{\longrightarrow} \frac{2}{\eta(s)} \quad (3b)$$

$\widetilde{\nu}$ is an adjustable number of order unity, related to the ultraviolett cutoff k_ξ of the theory [32]. $\eta^{(i)}_{\rm eff}(s)$ is the local effective viscosity, i.e. Eq. (2), averaged over a coarse-graining volume, centered around $\mathbf{r}_i$. $\langle \dots \rangle_i$ denotes an average with respect to the local energies E_i. The explicit form of $\eta^{(i)}_{\rm eff}$ is

$$\frac{1}{\eta^{(i)}_{\rm eff}(E,s)} = \frac{1}{\eta_0} e^{-\beta_{\rm eff}E} + \frac{sV}{E} \quad (4)$$

We emphasize that in the very high frequency regime, where viscous effects become irrelevant, our theory reduces to heterogeneous elasticity theory [26, 32], which describes the high-frequency vibrational anomalies of glasses associated with the boson peak (see the discussion of Eqs. (8) - (10) and Fig. 2 at the end of this article). This means that the present theory describes both dynamical and vibrational heterogeneities.

As we want to compare in the following the behavior of the heterogeneous viscosity with diffusive single-particle motion in the same energy landscape, (heterogeneous diffusivity) in the $\omega \to 0$ limit, we quote the CPA equations for this problem from Köhler et al. [32]:

$$D(s) = \left\langle \frac{D^{(i)}}{1 + \frac{\widetilde{\nu}}{3}\big(D^{(i)}(s) - D(s)\big)\Lambda_D(s)} \right\rangle_i \quad (5)$$

with $\Lambda_D(s) = \frac{3}{k_\xi^3}\int_0^{k_\xi} dk k^4 [s + D(s)k^2]^{-1}$ Here $D(s)$ is the dynamic diffusivity and $D^{(i)} = D_0 e^{-\beta_{{\rm eff},D}E^{(i)}}$ are the local diffusivities with $\beta_{{\rm eff},D} = [k_BT]^{-1} - \alpha_D$ [39].

In the $s \to 0$ limit $\Lambda_\eta \to 2/\eta(s=0) \equiv 2/\eta$ and $\Lambda_D \to 1/D(s=0) \equiv 1/D$, and we obtain for the $\omega \to 0$ limit of the viscosity and diffusivity the CPA equations

$$\frac{2\widetilde{\nu}}{3} = \int_0^\infty dE P(E) \frac{1}{\big(\frac{3}{2\widetilde{\nu}} - 1\big)\frac{\eta}{\eta^{(i)}} + 1} \quad (6a)$$

$$\frac{\widetilde{\nu}}{3} = \int_0^\infty dE P(E) \frac{1}{\left(\frac{3}{\widetilde{\nu}} - 1\right)\frac{D}{D^{(i)}} + 1} \qquad (6b)$$

If the macroscopic viscosity and diffusivity are parametrized as $\eta \propto e^{\beta_{\rm eff}\mu_\eta}$, $D \propto e^{-\beta_{\rm eff,D}\mu_D}$, the integrands in Eqs. (6a) and (5b) become step functions $\theta(E-\mu_\eta)$ and $\theta(\mu_D - E)$, resp. in the low-temperature limit, and we arrive at

$$1 - \frac{2\widetilde{\nu}}{3} = \int_0^{\mu_\eta} dE P(E) \qquad \frac{\widetilde{\nu}}{3} = \int_0^{\mu_D} dE P(E) \qquad (7)$$

This means that (within CPA) both the diffusivity and viscosity with spatially fluctuating activation energies acquire an Arrhenius behavior, independently of the details of $P(E)$. This result is well known for the diffusivity and (for charged carriers) conductivity in disordered materials [32, 40]. It reflects the fact that the carrier look for a path of minimum resistance through the material, which is a percolation path. In the percolation theory of hopping conduction [40] the number $\widetilde{\nu}/3$ is the continuum percolation threshold, which we now call p_D. The analogous quantity for the viscosity is $p_\eta = 1 - 2p_D$, where the factor 2 can be traced back to the two transverse cartesian degrees of freedom of the shear motion [32]. As pointed out in Köhler et al. [32], Eq. (5b) is also equivalent to an effective-medium theory for a conductance network, where the parameter p_D is $2/Z$, Z being the functionality of the network. So we note the result that except for the special case $p_D = 1/3$ the activation energy for diffusion and viscosity should be different. The explanation is that the percolation process for a single-particle and cooperative motion in three dimension is different. This is nicely described by the CPA in the $\omega \to 0$ limit. If we take for $p_D = \widetilde{\nu}/3$ the three-dimensional continuum percolation threshold ≈ 0.3 we arrive at $p_\eta = 1 - 2p_D = 0.4$. Using Eqs. (7) we arrive for a Gaussian distribution centered at E_0 with width parameter $\sigma/E_0 = 0.3$ at $\mu_D/E_0 = 0.843$ and $\mu_\eta/E_0 = 0.925$, i.e. the ratio is $\mu_D/\mu_\eta = 0.91$. This ratio (Einstein-violation parameter) depends on dimensionality through p_D, but it is non-universal, as it depends on (and becomes smaller with) the shape of the distribution.

We now turn to the finite-frequency regime. This is the regime around and above the alpha peak. In this frequency regime the function $\Lambda_\eta(s)$ can be replaced by its low-frequency limit $\Lambda_\eta(s) = \frac{2}{\eta(s)}$. Below the alpha peak the shear loss modulus is just given by $G'' = \omega\eta(0)$, which describes the linear increase of G'' below the α peak. Such a behavior is (to the best of our knowledge) obeyed in all mechanical relaxation data [41].

As stated above, the frequency-dependent viscosity $\eta(s)$ depends on the detailed shape of $P(E)$. As we want to compare our theory with mechanical relaxation data in metallic glasses, we believe that a good choice for this function is a Gaussian, truncated at $E = 0$ [42], i.e. $P(E) = P_0\theta(E)e^{-(E-E_0)^2/2\sigma^2}$, because the local shear moduli in simulations of metallic [43, 44] and other glasses with soft-sphere interaction [25, 45, 46] were

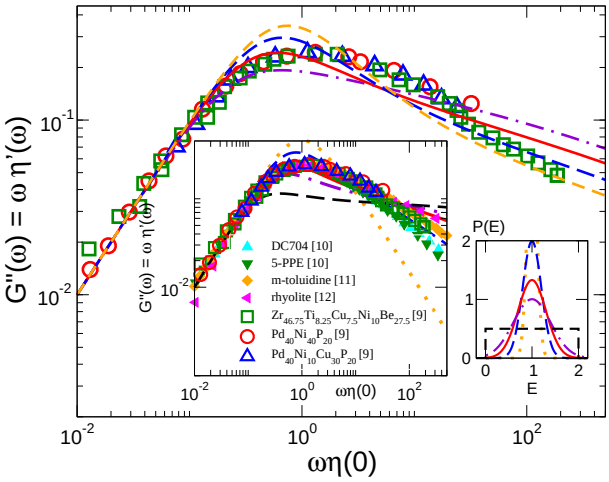

FIG. 1: Main body: Relaxation curves $G''(\omega) = \omega\eta'(\omega)$ vs. $\omega\eta(0)$ for Gaussian distributions with width $\sigma/E_0 = 0.3$ and effective inverse temperatures $\beta_{\rm eff}E_0 = 24$ (violet dash-dots), 26 (red continuous line), 28 (blue long dashes) and 30 (orange short dashes). The open symbols are representative data of three bulk metallic glasses compiled by Wang et al. [9]. For the percolation threshold we used $\widetilde{\nu}/3 = 0.3$.
Big inset: Same as in the main body but for fixed inverse temperature $\beta_{\rm eff}E_0 = 26$ and varied widths $\sigma/E_0 = 0.1$ (orange dots), 0.2 (blue long dashes), 0.3 (red continuous line, same as in the main body) and 0.4 (violet dash-dots). The black short-dashed curve has been obtained with a flat distribution P(E)=0.5 for $0 \leq$ E ≤ 2. We included relaxation data of non-metallic organic and anorganic glasses (full symbols) [10–12]. The full chemical formulae of the organic glasses are tetraphenyl-tetramethyl-trisiloxane (DC704) and 5-phenyl-4-ether (5-PPE).
Small inset: The distribution densities $P(E)$ used for the calculations of the big inset. Color and line codes are the same for the two insets.

shown – by evaluating the statistics – to exhibit a Gaussian distribution. In Fig. 1 we show the loss modulus $G''(\omega) = \eta'(\omega)\omega$ as a function of the rescaled frequency $\widetilde{\omega} = \omega\eta(0)$. If the main ($\alpha$) relaxation peak remains near $\widetilde{\omega} = 1$, this means that the time-temperature superposition principle is obeyed. We compare our calculations for various values of the effective inverse temperature and parameter $\beta_{\rm eff}E_0$ and σ/E_0 with a recent compilation of relaxation data of bulk metallic glasses near the calorimetric glass transition T_g [9]. In order to demonstrate the robustness of the results with respect to the shape of $P(E)$ we included also a flat distribution $P(E) = 0.5\theta\big(E[2-E]\big)$. We see that the data fit best to $\beta_{\rm eff}E_0 = 26$ and σ/E_0 =0.3. As the activation energies of the viscosity for bulk metallic glasses are in the 3 eV range and the glass transition is around 700 K [47], we arrive at a relative inverse temperature of $E_a/k_BT \approx 50$, which leaves for the Meyer-Neldel entropy parameter a value of $\alpha/E_A \approx 24$, where we used our CPA result $E_a/E_0 \approx 1$. In the inset of Fig. 1 we show also relaxation data of two organic glasses [10] one anorganic glass

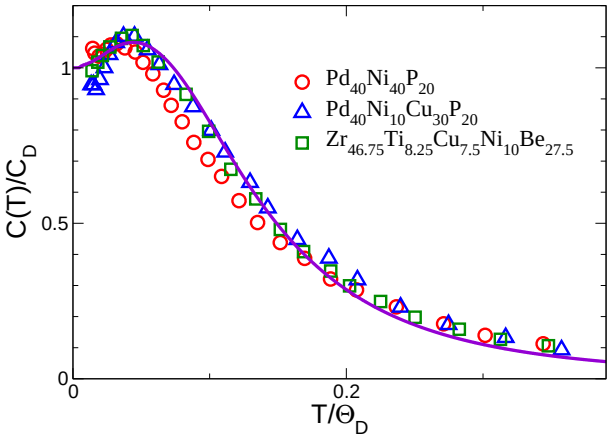

FIG. 2: Reduced specific heat $C(T)/C_D(T) \propto C(T)/T^3$ for three bulk metallic glasses [48], compared with the prediction of heterogeneous-elasticity theory, Eqs. (8) - (10) with a Gaussian distribution of shear moduli $\sigma_G/G_0 = \sigma/E_0 = 0.3$. For the ratio between the Debye and correlation cutoff we used $k_D/k_\xi = 1.6$ and for the re-scaling of the experimental temperature scale we used the Debye temperatures Θ_D = 278 K ($Pd_40Ni_40P_20$), 280 K ($Pd_40Ni_10Cu_30P_20$), 320 K ($Zr_46.75Ti_8.25Cu_7.5Ni_10Be_27.5$)

[11], and one highly disordered mineral [12] in order to demonstrate the generality of our approach.

In the beginning we mentioned that at high frequency our theory becomes equivalent to the CPA version of heterogeneous-elasticity theory [26, 32], which explains the boson-peak-related glassy vibrational anomalies in the THz range. In this regime the viscosity term in Eq. 2 is negligible, leaving the fluctuating shear modulus $G(\mathbf{r}_i) \equiv G^{(i)}$. In terms of the frequency-dependent shear modulus $G(s) = s\eta(s)$ and the susceptibility function $\Lambda_G(s) = \Lambda_\eta(s)/s$ the CPA equation (3a) takes the form

$$G(s) = \left\langle \frac{G^{(i)}(s)}{1 + \frac{\tilde{\nu}}{3}\big(G^{(i)}(s) - G(s)\big)\Lambda_G(s)} \right\rangle_i \qquad (8)$$

from which we can calculate the density of vibrational states $g(\omega)$ and the specific heat $C(T)$ as

$$g(\omega) = \frac{2\omega}{3\pi}\mathrm{Im}\left\{\frac{3}{k_D^3}\int_0^{k_D} dk k^2 \left(\frac{1}{s^2 + \left[K + \frac{4}{3}G(s)\right]k^2} + \frac{2}{s^2 + G(s)k^2}\right)\right\} \qquad (9)$$

$$C(T) \propto \int_0^\infty d\omega\, g(\omega)(\omega/T)^2 \frac{e^{\hbar\omega/k_BT}}{[e^{\hbar\omega/k_BT} - 1]^2} \qquad (10)$$

Here k_D is the Debye wavevector. In Fig. 2 we show a calculation of the reduced specific heat $C(T)/C_D(T) \propto C(T)/T^3$ according to the CPA equations (8) to (8), together with experimental data of the same bulk metallic glasses referred to in Fig. 1. We used the same width-maximum relation $\sigma_G/G_0 = \sigma/E_0$ as in the calculations of the blue lines in Fig. 1. The other parameters are given in the caption. This calculation and the agreement to the data demonstrates that the same CPA theory can be used for the relaxation spectrum and the vibrational anomalies.

In conclusion we can state that we have established a combined theory for the $\omega \to 0$ limit of the viscosity, the low-temperature asymmetric α relaxation and the high-frequency vibrational anomalies within a unified framework. This has been achieved by assuming that the viscous and elastic coefficients of Maxwell's theory of viscoelasticity fluctuate in space according to a frozen distribution of activation barriers. We have found an explanation of the discrepance of the activation energies for diffusion and viscosity in terms of the different percolative properties of the two heterogeneous transport problems and a theory for the low-temperature alpha relaxation below the glass transition.

W. S. is grateful for helpful discussions with Th. Franosch, M. Fuchs, W. Götze, E. Rössler, F. Sciortino, T. Scopigno, R. Schilling, and Th. Voigtmann.

[1] J. C. Maxwell, Philos. Trans. Roy. Soc. London **157**, 49 (1867).
[2] J. C. Dyre, N. B. Olsen, and T. Christensen, Phys. Rev. B **53**, 2171 (1996).
[3] J. C. Dyre, Rev. Mod. Phys. **76**, 953 (2006).
[4] T. Hecksher, J. C. Dyre, J. Non-Cryst. Solids **407**, 14 (2015).
[5] K. Samwer and W. L. Johnson, Phys. Rev. Lett. **95**, 195501 (2005).
[6] A. C. Angell, J. Non-Cryst. Solids **131**, 13 (1991).
[7] A. C. Angell, Nature **410**, 663 (2001).
[8] G. P. Johari and M. Goldstein, J. Chem. Phys. **53**, 2372 (1970).
[9] L.-M. Wang, R. Liu, and W. H. Wang, J. Chem. Phys. **128**, 164502 (2008).
[10] T. Hecksher et al., J. Chem. Phys. **138**, 12A543 (2013).
[11] S. A. Hutcheson and G. B. McKenna, J. Chem. Phys. **129**, 074502 (2008).
[12] S. Webb, Rev. Geophys. **35**, 191 (2000).
[13] J. Wong and C. A. Angell, *Glass : structure by spectroscopy* (M. Dekker, 1976).
[14] U. Bengtzelius, W. Götze, and A. Sjölander, J. Phys. C **17**, 5915 (1984).
[15] W. Götze, in *Liquids, Freezing and the Glass Transition*, edited by J. P. Hansen, D. Levesque, and J. Zinn-Justin (Elsevier, Amsterdam, 1991).
[16] W. Götze, *Complex Dynamics of Glass-Forming Liquids* (Oxford Univ. Press, Oxford, 2009).
[17] E. Rössler, Phys. Rev. Lett. **65**, 1595 (1990).
[18] F. Fujara et al., Z. Phys. B **88**, 195 (1992).
[19] M. Goldstein, J. Chem. Phys. **51**, 3728 (1969).
[20] F. H. Stillinger, Science **267**, 1935 (1995).

[21] P. G. Debenedetti and F. H. Stillinger, Nature **410**, 259 (2001).
[22] C. A. Angell et al., J. Phys. Condens. Matter **15**, S1051 (2003).
[23] W. Schirmacher, Europhys. Lett. **73**, 892 (2006).
[24] W. Schirmacher, G. Ruocco, and T. Scopigno, Phys. Rev. Lett. **98**, 025501 (2007).
[25] A. Marruzzo, W. Schirmacher, A. Fratalocchi, and G. Ruocco, Nature Scientific Reports **3**, 1407 (2013).
[26] W. Schirmacher, T. Scopigno, and G. Ruocco, J. Non-Cryst. Solids **407**, 133 (2015).
[27] K. Gilroy and W. A. Phillips, Philos. Magazine B **43**, 735 (1981).
[28] J. C. Dyre and N. B. Olsen, Phys. Rev. Lett. **91**, 155703 (2003).
[29] T. Voigtmann and T. Rizzo (2014), arXiv:1403.2764v2.
[30] S. Kirkpatrick, Rev. Mod. Phys. **45**, 574 (1973).
[31] R. J. Elliott, J. A. Krumhansl, and P. L. Leath, Rev. Mod. Phys. **46**, 465 (1974).
[32] S. Köhler, R. Ruocco, and W. Schirmacher, Phys. Rev. B **88**, 064203 (2013).
[33] B. Charbonneau et al., J. Chem. Phys. **139**, 164502 (2013).
[34] A. Yelon and B. Movaghar, Phys. Rev. Lett. **65**, 618 (1990).
[35] A. Yelon, B. Movaghar, and R. S. Crandall, Rep. Prog. Phys. **69**, 1145 (2006).
[36] R. W. Keyes, J. Chem. Phys. **29**, 467 (1958).
[37] A. W. Lawson, J. Chem. Phys. **32**, 131 (1960).
[38] For simplicity reasons we do not take fluctuations of K and bulk viscosity effects into account. Such effects can be incorporated easity.
[39] For the diffusivity a local Meyer-Neldel compensation rule should also hold, but, of course, the coefficient α_D need not be the same as that for the viscosity.
[40] A. I. Efros and B. I. Shklovskiĭ, *Electronic properties of doped semiconductors* (Springer-Verlag, Heidelberg, 1984).
[41] One should be careful not to compare the predictions for $G''(\omega)$ with dielectric relaxation data. They are rather related to the imaginary part of the susceptibility $\chi(\omega) \propto G(\omega)^{-1}$.
[42] As can be seen from the second inset in Fig. 2, the lower cutoff in the distribution density $P(E)$ at $E = 0$ is not relevant for the chosen width parameters σ/E_0.
[43] S. G. Mayr, Phys. Rev. B **79**, 060201 (2009).
[44] P. M. Derlet, R. Maass, and J. F. Löffler, Eur. Phys. J. **85**, 148 (2012).
[45] H. Mizuno, S. Mossa, and J.-L. Barrat, Phys. Rev. E **87**, 042306 (2013).
[46] H. Mizuno, S. Mossa, and J.-L. Barrat, Europhys. Lett **104**, 56001 (2013).
[47] E. Bakke, R. Busch, and W. L. Johnson, Appl. Phys. Lett. **67**, 3260 (1995).
[48] Y. Li, P. Yu, and H. Y. Bai, J. Applied Phys. **104**, 013520 (2008).